Revista de Chimie
https://revistadechimie.ro
https://doi.org/10.37358/Rev. Chim.1949

Response of Kostiakov-Lewis Infiltration Parameters to Soil Physical-Chemical Properties in the Loess Plateau of China

WENJING QIN, GUISHENG FAN*
College of Water Resources Science and Engineering, Taiyuan University of Technology, Shanxi 030024, China

Abstract: *In order to know the main factors influence the infiltration parameters, based on the 344 sets of double-ring infiltration experiments in 101 different experimental sites in the Loess Plateau, obtained a large sample of Kostiakov-Lewis infiltration model parameters, analyzed the relationship between infiltration parameters and soil properties, established a multiple linear model, a nonlinear model and a BP neural network model to predict the infiltration parameters. The results showed that through Pearson correlation analysis, the main factors for parameter k was bulk density, soil water content of 0-10 cm, sand content, silt content and organic matter of 0-20 cm, the main factors influence parameter α was water content, sand content, silt content of 0-40 cm, and bulk density of 20-40 cm, and the main factors for parameter f0 was water content, sand content, silt content, of 0-40 cm, bulk density of 10-40 cm, and organic matter of 0-20 cm. Compared with previous studies, this paper added soil organic matter content as an independent variable to study the effect of soil chemical properties on soil infiltration capacity, which makes the model more reasonable, higher accuracy, and better prediction effect. Based on the effective test, result error analysis and comprehensive analysis, it was feasible to obtain the infiltration parameters in the Kostiakov-Lewis model using three Pedo-transfer functions. Under the condition of comprehensive consideration of forecast accuracy and stability applicability, it was recommended to use the nonlinear model as the prediction model of soil water infiltration parameters in the Loess Plateau.*

Keywords: *Soil physical and chemical properties; Kostiakov-Lewis infiltration model; Pearson correlation analysis; soil organic matter content; multiple linear model; nonlinear model; BP neural model*

1. Introduction

The Loess Plateau region is located in the north-central part of China. It belongs to the temperate monsoon climate, with less rainfall and uneven rainfall, lack of water resources and drought. Therefore, the acquisition of soil water infiltration parameters is a fundamental problem in the climate and environment management in this region.

Soil water infiltration refers to the process of water infiltration into the soil through the surface and stored in the soil under irrigation or rainfall conditions. At present, the models describing soil water infiltration process mainly include Green-Ampt model [1], Kostiakov model [2], Philip model [3], Horton model [4] and so on. Regardless of the application of the model, it depends on the determination of the model parameters. The methods for obtaining the infiltration model parameters include the direct method and the indirect method. The direct method includes laboratory test method and field test method. The indirect method includes field irrigation process method and soil Pedo-transfer function method. The laboratory test method has great differences with the field soil in the construction of soil water infiltration model, and there are differences between the experimental and the actual irrigation parameters. The field test method uses special equipment to test the soil water infiltration process in the field, the double-ring infiltration instrument is most commonly used, but the method has a long measuring time and the process is complicated. The field irrigation process refers to the determination of soil infiltration parameters using irrigation data, including the two-point method of Kostikov-Lewis model [5], the Philip model one-point method [6], the M method [7], the M-J

*email: fan.g161@yahoo.com, tyutfanguisheng@126.com

method [8], and the M-Z method [9], etc. These test methods have a large workload, a complicated implementation process, and a long time-consuming process, and the estimated values of the infiltration parameters are average values. In comparison, the soil Pedo-transfer function method [10] is based on the basic physical and chemical parameters and obtains the soil infiltration parameters through the transfer function model. The method is simple in operation, low in test cost, short in test time, and therefore widely used in obtaining hydraulic parameters. Many experts and scholars use the Pedo-transfer function to predict soil water characteristic curve [11, 12], soil characteristic water content [13-15], soil bulk density [16, 17], and soil organic carbon content [18-20]. However, there are few predictions of soil water infiltration parameters [21-38].

Based on the series of infiltration experiments of farmland scale in the Loess Plateau, this paper fits a large sample of Kostiakov-Lewis infiltration model parameters and related soil physical and chemical parameters and adopts multiple linear, nonlinear and BP neural network methods to establish the Pedo-transfer functions between each infiltration parameter and soil properties. The prediction of soil water infiltration model parameters is realized, which provides technical support for agricultural water resources management in the Loess Plateau.

2. Materials and methods

2.1. Soil conditions in the test area

The test area was located in the Loess Plateau of China, centered on Shanxi Province. The test area was 600km from north to south and 400km from east to west. The test points were distributed in the topography units such as mountains, hills, and floodplains. The soil bulk density varied from 0.89 to 1.762 g/cm^3; the soil volumetric moisture content ranged from 2.0 to 45.2%; the soil organic matter content ranged from 0.416 to 6.60 g/kg, and the basic physical and chemical properties of the soil were shown in Table 1. The test area basically covers various soil types in the Loess Plateau, and the soil physical and chemical parameters varied greatly, which better represented the loess soil condition in the Loess Plateau.

Table 1. The basic physical and chemical properties of the soil

Soil properties	variation range	Soil properties	variation range
0~10cm Soil Bulk Density γ_0 (g/cm^3)	0.890~1.588	0~20cm Silt content δ_2 (%)	0.053~0.760
10~20 cm Soil Bulk Density γ_1 (g/cm^3)	0.964~1.562	0~20cm Clay content δ_3 (%)	0.008~0.235
20~40 cm Soil Bulk Density γ_2 (g/cm^3)	0.774~1.762	20~40cm Sand content δ_4 (%)	0.096~0.930
0~10cm Volumetric water content θ_1(%)	0.020~0.452	20~40cm Silt content δ_5 (%)	0.441~0.850
10~20cm Volumetric water content θ_2 (%)	0.0241~0.328	20~40cm Clay content δ_6 (%)	0.009~0.331
20~40cm Volumetric water content θ_3 (%)	0.030~0.422	0~20cm Organic matter G (%)	0.416~6.589
0~20cm Sand content δ_1 (%)	0.097~0.880		

2.2. Test methods

The combination of field test and laboratory test was used to obtain soil infiltration characteristics and soil physical and chemical properties at different test points.

(1) Field test: The soil double-ring infiltration instrument was used for the soil water infiltration test. The inner and outer rings have a diameter of 26 and 64 cm, respectively, and the height of both rings was 25 cm. Before the test, the double-ring of the infiltration instrument was buried vertically in the soil at 20 cm. During the test, use 50-1000ml measuring cylinder, slowly add tap water to the inner ring of the infiltration instrument in a period of time, ensure that it would not impact the surface soil during the adding process, and make sure the infiltration head of the whole test process always through

the self-made water level controller. The infiltration head was maintained at around 2 cm, tap water in the test area was used for the entire test process. After the start of the test, the soil water infiltration time and the infiltration amount were recorded in different time periods. Record once every 1 min in the first 8 min after the start of the test, once every 2 min in 10-15 min, once every 5 min in 15~60 min, and once every 10 min after 60 min. The test time was extended to 90 minutes in consideration of the reliability of the test.

(2) Laboratory test: Undisturbed soil cores were taken at each site in 0-10cm, 10-20cm, 20-40 cm using mental cylinders (100 cm^3) to measure bulk density (BD) and the initial water content. Oven-dried the soil cores at 105 ℃ for 48 hours, then weighted to calculated BD and initial water content. The disturbed soil samples (0-20 and 20-40 cm) were air-dried and passed through 2mm mesh to measure the sand (0.02-2 mm), silt (0.002-0.02 mm), clay (＜0.002 mm) content using sifting curve method, and the soil organic matter (SOM, 0-20 cm) was tested using the dichromate oxidation method.

2.3. Research methods

2.3.1. Fitting of Parameters of Soil Water Infiltration Model

The soil infiltration model is a relationship between the soil water infiltration and the infiltration time. It can quantitatively or qualitatively analyze the soil infiltration process, thus revealing the soil infiltration law and providing mathematical means to study the process of soil water infiltration. Common soil water infiltration models include the Green-Ampt model, Kostiakov model, Philip model, Horton model and so on. A large number of studies have shown that Kostiakov-Lewis model has high fitting precision, close to the actual irrigation and infiltration of farmland, and has good applicability. It is the most commonly used empirical model for studying soil water infiltration. Therefore, this paper uses Kostiakov-Lewis model to describe the infiltration process of loess soil in the Loess Plateau. The Kostiakov-Lewis model is shown as follows.

$$I(t) = kt^{\alpha} + f_0 t \qquad (1)$$

where I (cm) is the cumulative infiltration per unit area, t (min) is the infiltration time, k (cm/min), α (non-dimensional), f0 (cm/min) are empirical parameters. f0 is the final infiltration rate at the steady state, when infiltration time is sufficient long.

Through the field double-ring infiltration test, different time t and cumulative infiltration amount I of the test point were obtained. The Matlab software CFtool toolbox was used for nonlinear fitting, and the optimal fitting parameters were obtained as the infiltration parameter values, namely the values of k, α, and f0. Then, the infiltration parameter value is corresponding to the physical and chemical parameter value, which constitutes the sample sequence, and the individual data with obvious errors are eliminated. Finally, 344 representative experimental data are selected as the experimental sample data set.

2.3.2. Estimation of the Infiltration Parameters to Soil Properties

The Pedo-transfer function is constructed to establish a functional relationship between soil water infiltration parameters and soil physical and chemical parameters such as soil bulk density, initial volumetric water content, sand content, silt content, clay content, and organic matter content, that is, PTFs. This paper mainly uses multiple linear model, nonlinear model, and BP neural network model to construct soil Pedo-transfer function.

(1) Multiple linear model: The multivariate linear model is realized by the linear regression relationship between the output parameters and the input parameter data, that is, the linear expression between the output parameters and the input parameters is determined by linear regression analysis between the test sample data sets. The model form is finally determined under the condition that the prediction accuracy is acceptable. The structure of the multiple linear model is as follows.

$$Y = \alpha_0 + \alpha_1 X_1 + \alpha_2 X_2 + \cdots + \alpha_n X_n \qquad (2)$$

where Y is the dependent variable, α_i is the model regression coefficient, X_i is the influencing factor, and n is the number of independent variables.

(2) Nonlinear model: When constructing a multivariate nonlinear model, firstly, the independent variables of each infiltration parameter are selected. According to the CFtool toolbox and the results of the mechanism analysis, the single factor function form of each variable is determined, and then the initial structure of the multivariate nonlinear soil transfer function is determined. Secondly, using Matlab software to perform multiple t-tests of independent variables, using 1stOpt software to perform multiple fittings, and performing significance test to establish a multivariate nonlinear prediction model. The model building process is shown in Figure 1.

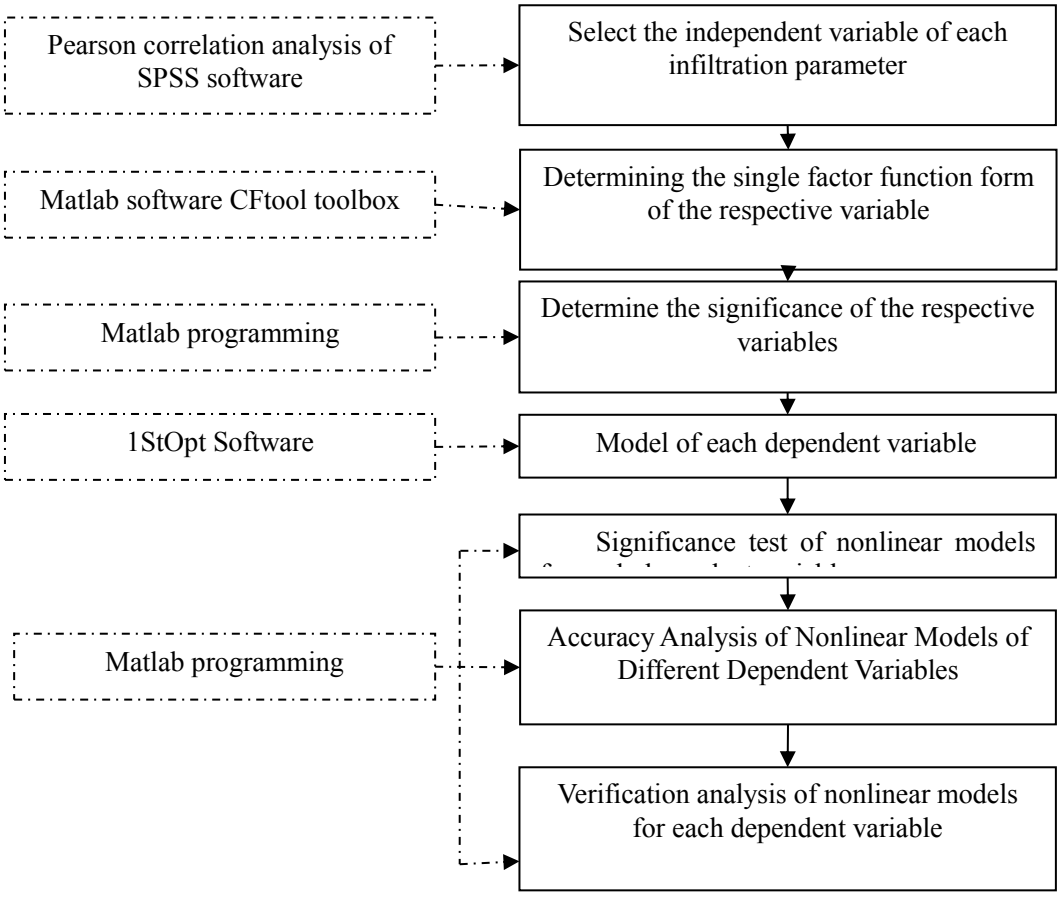

Figure 1. Nonlinear model construction flow chart

(3) BP neural network model: The BP neural network model is a multi-layer forward neural network model based on the error backpropagation algorithm. The model has a strong nonlinear mapping ability. Based on the analysis of the correlation between independent variables and dependent variables, the hidden neural network model is set. The number of layers and the number of hidden layer nodes are included, thus realizing effective mapping of the nonlinear relationship between input parameters and output parameters. The BP neural network model structure is as follows.

Net = newff (minmax (traininput), [i,1],{'tansig','logsig','trainlm') (3)

where new ff is a function for establishing a feedforward neural network, minmax is the range of the sample, train input is the training input value, i is the number of hidden layer nodes, 1 is the number of output layer nodes, tensing is the activation function of the hidden layer, purelin is the activation

function of the output layer, and trainlm is the default training optimization function.

2.4. Data Processing and Software Used

The independent variables are determined by Pearson correlation analysis, and the significance test of the independent variables is performed by t-test with a confidence level of 0.05. A predictive model significance test was performed using a joint F test with a confidence level of 0.05. The comparison of the prediction models is mainly determined based on the residual square sum (RSS), the Pearson correlation coefficient (P-R), the deterministic coefficient (R2), the relative error (RE), and the mean relative error (MRE). Where RE is calculated as follows.

$$RE = \left| \frac{y_i - \hat{y}_i}{y_i} \right| \quad (4)$$

$$MRE = \frac{\sum_{i=1}^{N} RE}{N} \quad (5)$$

where y_i is the measured value, $\hat{y}_i$ is the predicted value, and N is the number of samples. The residual square sum (RSS), the Pearson correlation coefficient (P-R), the deterministic coefficient (R2) of the predicted and measured values are obtained by linear regression of Origin 8.0 software.

Sample Pearson correlation analysis iss performed using IBM SPSS Statistics 22 software. A multivariate linear model is built using IBM SPSS Statistics 22 software back regression analysis. A multivariate nonlinear model is established using 1StOpt and Matlab software. The BP artificial neural network model is established by Matlab software. Drawing with Origin 8.0.

3. Results and discussions

3.1 Soil infiltration Parameters Analysis

The infiltration parameter k is numerically equal to the difference between the cumulative infiltration amount and the stable infiltration rate at the end of the first unit period after the start of infiltration. The larger the k value, the larger the infiltration amount at the end of 1 min. During the test, as the soil water infiltration progresses, water enters the soil accompanied by immersion, collapsing, deformation and other processes of the surface soil, which means that the soil skeleton is deformed during the infiltration of soil water. The deformation trend is that the density of topsoil is changed from loose to dense, and the soil bulk density before and after infiltration is greatly different, which leads to the change of soil water infiltration capacity. The larger k value, the more unstable the soil structure, and the greater the soil deformation during the water infiltration process, which leads to an increase in the error between the predicted value and the measured value.

Since the parameter α reflects the decay rate of the infiltration capacity, the mechanism of the attenuation of the soil infiltration capacity is very complicated. At the beginning of soil water infiltration, the soil is dry, the molecular force is strong, the water is quickly adsorbed to form film water, and then the pores of the surface soil are filled, and the soil matrix potential becomes the motive force. Therefore, the α value is mainly determined by the initial moisture content and soil structure of the wet front. The initial infiltration rate of the soil is very fast. In a short period of time, the soil layer is basically saturated within a certain thickness range below the surface. With the extension of infiltration time, the cross-section of water passes from full-surface water in the initial period of infiltration to partial cross-section water. The infiltration gradient is reduced, the infiltration rate is slowed down, and the decay rate is slowed down.

When the soil reaches a stable infiltration rate, the water content of the topsoil (0~20 cm) is saturated water content, and the soil water potential gradient driving the infiltration water flow movement is 1. The relatively stable infiltration rate f0 is essentially the saturated water conductivity rate of the soil. At this time, the upper soil infiltration channel has basically formed, and the value of f0 mainly depends on the soil structure.

3.2. Response of Infiltration Parameters to Soil Properties

In the Kostiakov-Lewis model, k is the infiltration coefficient, indicating the infiltration rate in the first period of soil water infiltration, which is mainly related to the initial state of the soil. Therefore, the physicochemical properties of the soil in 0~20 cm can be selected as input parameters. α is the infiltration index, indicating the decay rate of infiltration performance, which is related to the whole irrigation process. It is necessary to consider the physical and chemical properties of the tillage layer (0-20 cm) and the plow bottom layer (20~40 cm). f0 is a relatively stable infiltration rate, indicating the infiltration parameter when the soil infiltration reaches a relatively stable state, which is related to the soil properties after stabilization. The physical and chemical properties of the tillage layer and the plow bottom soil can be considered as input parameters. Considering the linear relationship between sand, silt and clay content in the soil, it is only necessary to select two or one of them as input parameters. In this paper, Pearson correlation analysis was performed with SPSS using the selected 344 data samples. The results are shown in Table 2.

Table 2. Pearson correlation analysis between the infiltration parameters and soil properties

Soil properties	k	a	f_0
γ_0	-0.613**	-0.052	-0.011
γ_1	-0.042	0.071	-0.179**
γ_2	-0.117	0.132*	0.264**
θ_1	0.214**	-0.225**	-0.299**
θ_2	0.014	-0.349**	-0.306**
θ_3	-0.074	-0.125*	-0.375**
δ_1	-0.442**	0.223**	0.166*
δ_2	0.376**	-0.224**	-0.205**
δ_3	0.077	-0.073	-0.006
δ_4	-0.042	0.204**	0.153*
δ_5	0.075	-0.278**	-0.141*
δ_6	0.063	-0.94	-0.016
G	-0.441**	-0.083	0.292**

According to the Pearson correlation test result, soil properties γ0 and δ1 had negative effect in parameter k. soil properties θ1 and G had positive effect in parameter k. soil properties θ1, θ2, θ3, δ2 and δ5 had negative effect in parameter α. soil properties γ2, δ1 and δ4 had positive effect in parameter α. soil properties γ1, θ1, θ2, θ3, δ2 and δ5 had negative effect in parameter f0. soil properties γ2, δ1, δ4 and G had positive effect in parameter f_0.

Soils with different organic matter content have different distribution of soil pores. Soils with high organic matter content have good soil structure and many medium pores; on the contrary, soils with low organic matter content have poor soil structure and have very large pores or small pores. In the early stage of soil infiltration, the large pores are mainly filled first. The water seeps into the lower layer by its gravity, and the soil with extra large pores has a large infiltration capacity. Therefore, the soil with low organic matter content has a large infiltration capacity in the early infiltration period, and the soil with a high organic matter content has a relatively small infiltration amount in the early infiltration period. Therefore, the *k* value decreases with increasing soil organic matter content.

Soils with low organic matter content have poor soil structure or poor granular structure stability. After encountering water, some granules on the surface are likely to collapse and become more uniform small particles. During the process of soil infiltration, the dissolved silt particles tend to be deposited in some large pores to hinder the infiltration of water, the dissolved clay particles accumulate on the surface of the soil, forming a thin dense layer, correspondingly hindering the infiltration of water, the amount of soil infiltration decreases, so the soil infiltration speed decays fast. On the contrary, in soils with high organic matter content, the soil aggregate structure is more and stable, and the aggregate structure is not easy to collapse after encountering water, and it is not easy to form a dense layer on the ground surface, and the amount of water infiltration is relatively large, so the

soil infiltration rate and soil infiltration capacity decay slowly. Therefore, the infiltration index α decreases with increasing soil organic matter content.

There is a significant positive correlation between the content of organic matter and f_0. The analysis believes that the content of organic matter can reduce the bulk density of the soil and increase the soil pores, thereby improving the soil water conductivity, resulting in an increase in f_0 value.

3.3. Estimation of Infiltration Parameters to Soil Physical-Chemical Properties

3.3.1. Model Construction

In order to obtain the infiltration parameters, the multiple linear, nonlinear and BP artificial neural network prediction models were constructed. The model are shown in Table 3.

Table 3. Pedo-transfer functions

Methods	Pedo-transfer functions
Multiple linear model	$k = 5.118 - 5.528\theta_1 - 2.456r_0 + 2.043\omega_2 - 0.398G$ $\alpha = 0.162 - 0.259\theta_1 - 0.47\theta_2 - 0.131\gamma_2 + 0.326\omega_1 + 0.448\omega_2$ $f_0 = 0.071 - 0.21\theta_2 - 0.204\theta_3 + 0.046G + 0.076\omega_5 - 0.109\omega_6$
Nonlinear model	$k = 0.284 + 1.960e^{-7.820\theta_1} + 6.694\gamma_1 + 1.659\,ln\,\delta_2 - 8.172e^{14.525G}$ $\alpha = 0.338 + 0.093\,ln\,\theta_1 - 0.998\theta_1 - 0.050\,ln\,\theta_2 - 0.023\theta_2 - 0.219\gamma_1 + 0.090r_2 + 0.219\delta_1 + 0.396\delta_2 + 0.030\,ln\,\mathrm{G}$ $f_0 = 0.204 + 0.001e^{10.340\theta_1} - 0.232e^{1.008\theta_2} + 0.030\,ln\,G + 0.073e^{-10.528\theta_3} + 0.096\delta_4 + 0.167\delta_5$
BP neural network model	*k: net=newff(minmax(traininput),[i,1],{'tansig','logsig'},'trainlm')* *α:net=newff(minmax(traininput),[i,1],{'tansig','logsig'},'trainlm')* *f_0: net=newff(minmax(traininput),[i,1],{'tansig','logsig'},'trainlm')*

The significance test of the predictive model independent variables was performed according to the t-test. Based on test results in Table 4, the t-values of the multivariate linear model and the nonlinear model are both greater than t0.05/2, indicating that the two independent predictive models have significant effects on the infiltration parameters. This result is consistent with the Pearson correlation test in 3.2.

Table 4. t-test for predicting model independent variables

Parameters	Multiple linear model		Nonlinear model		$t_{0.05/2}$
k	θ_1	-10.147	$e^{-7.820\theta_1}$	10.841	1.96
	γ_0	-6.910	γ_0	16.6036	
	δ_2	4.177	ω_2	5.0287	
	G	-2.146	$e^{14.525G}$	3.3377	
α			$ln\theta_1$	4.5630	
			θ_1	4.8552	
	θ_1	-2.135	$ln\theta_2$	4.7604	
	θ_2	-4.192	θ_2	4.8743	
	γ_2	-1.438	γ_1	2.8802	
	δ_1	2.224	γ_2	4.5008	
	δ_2	4.306	δ_1	3.2290	
			δ_2	5.1310	
			lnG	1.9936	
f_0	θ_2	-3.291	$e^{10.34\theta_1}$	2.3157	
	θ_3	-3.973	$e^{1.008\theta_2}$	11.8419	
	G	4.603	lnG	3.9826	
	δ_5	2.156	$e^{-10.528\theta_3}$	4.7001	
	δ_6	-3.252	δ_4	3.3584	
			δ_5	6.1606	

The three models established by 344 sets of samples was tested for significance, that is, by the joint F test, the corresponding F0.05 was obtained at a given significant level α (α=0.05). Calculate the F value of the prediction model, compare the F value and F0.05, and discriminate the significance of the prediction model. The test results are shown in Table 5. It show that the prediction results of the infiltration parameters k, α, and f0 are significantly using the three models.

Table 5. Significant test results of Pedo-transfer function

Parameters	F value					
	Multiple linear model	$F_{0.05}$	Nonlinear model	$F_{0.05}$	BP neural network model	$F_{0.05}$
k	31.47	2.404	87.221	2.404	347.51	2.247
α	19.82	2.247	118.355	1.914	503.47	1.94
f_0	38.31	2.247	205.528	2.132	862.25	1.94

3.3.2. Model Evaluation

(1) Effectiveness Analysis: Based on the independent variable significance test and the model significance test, the forms of the three models are finally determined (Table 3). The respective variable values are input into the model, and the fitted values of the infiltration parameters k, α, and f0 are obtained and compared with the measured values (Figure 2). The residual sum of squares (RSS), the Pearson correlation coefficient (P-R), and the deterministic coefficient (R2) between the predicted value and the measured value are shown in Table 6.

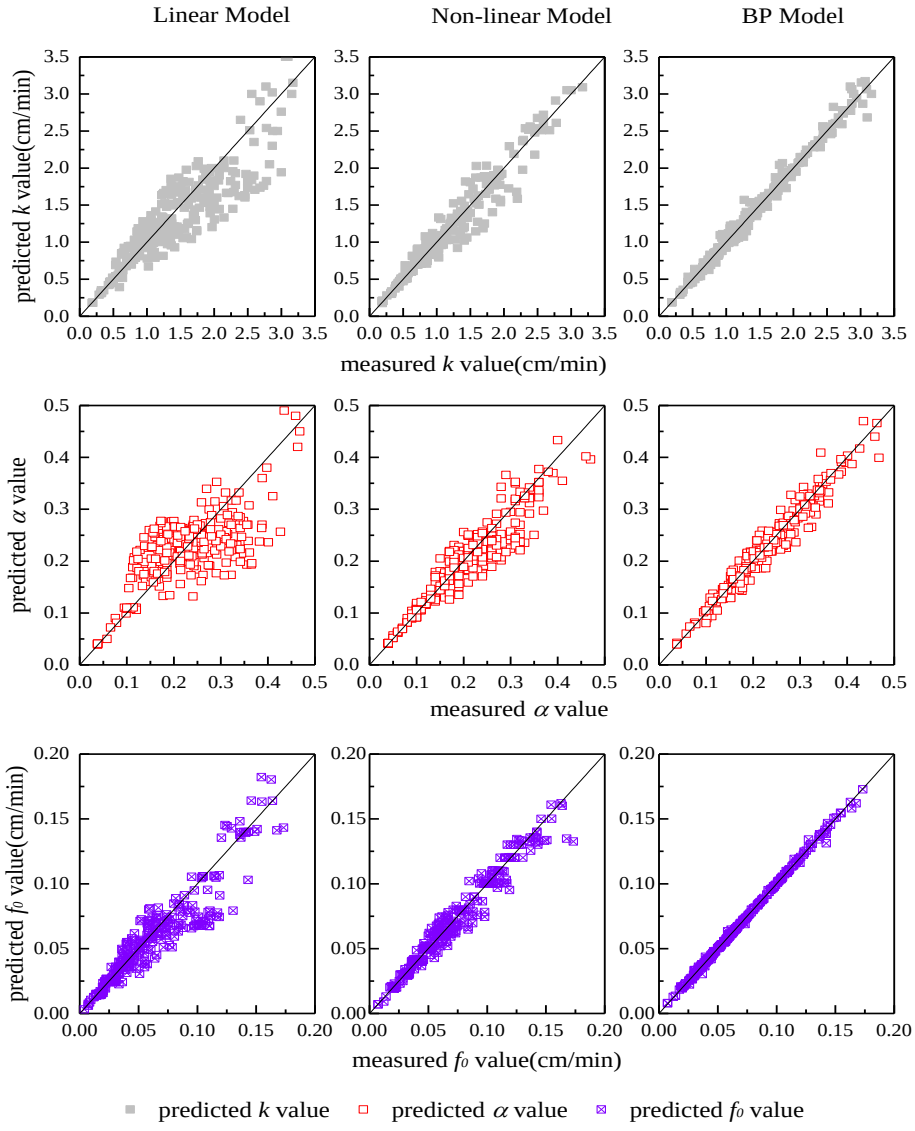

Figure 2. The measured and the predicted values of samples

Table 6. RSS, P-R and R values between the measured and predicted values of the infiltration parameters of the sample

Parameters	Multiple linear model			Nonlinear model			BP neural network model		
	RSS	*P-R*	R^2	*RSS*	*P-R*	R^2	*RSS*	*P-R*	R^2
k	9.3481	0.8969	0.8045	5.0593	0.9755	0.9516	1.4744	0.9944	0.9888
α	20.5689	0.6814	0.4643	7.2065	0.8418	0.8869	1.0797	0.9777	0.9560
f_0	7.4281	0.8124	0.8738	5.3721	0.9348	0.9036	0.00005	0.9992	0.9985

**RSS* is the residual sum of squares, *P-R* is the Pearson correlation coefficient, R^2 is the deterministic coefficient.

The three models constructed can better predict the three infiltration parameters. When multivariate linear model is used to predict the infiltration parameters of samples, the RSS value between the measured value and the predicted value is 3.56896-20.34808, the P-R coefficient is 0.68139-0.87382, and the R2 is 0.4643-0.87382. When using the nonlinear model to predict the infiltration parameters of the samples, the RSS value between the measured value and the predicted value is 2.20654-5.05934, the P-R coefficient is 0.9348-0.97553, and the R2 is 0.88695-0.95167. When the BP neural network model is used to predict the infiltration parameters of the samples, the RSS value between the measured value and the predicted value is 1.4744-0.0005, the P-R coefficient is 0.97775-0.99922, and the R2 is 0.956-0.99845.

The prediction effect of the infiltration parameter f0 of the sample by three methods (RSS value is 7.4218-0.0005, PR coefficient is 0.8124-0.99922, R2 is 0.87382-0.99845) is better than the infiltration parameter k (RSS value is 1.4744-9.34808, PR The coefficient is 0.889698-0.99443, R2 is 0.80458-0.98889), and is superior to the infiltration parameter α (RSS value is 1.07978-20.56896, PR coefficient is 0.68139-0.94445, R2 is 0.4643-0.956). According to the analysis, in the initial stage of infiltration, the infiltration process is greatly affected by various physical and chemical properties, and as the infiltration process progresses, the physical and chemical properties also change. When the infiltration parameter f0 is measured, the infiltration process is in a stable phase that is consistent with Rahmati results [39].

For the infiltration parameter k of the sample, the BP artificial neural network model has the lowest RSS value (1.4744), the largest P-R value (0.99443), and the largest R2 (0.98889), and the fitting effect is optimal. For the infiltration parameter α of the sample, the BP artificial neural network model has the lowest RSS value (1.07978), P-R maximum (0.97775) and R2 maximum (0.956), and the fitting effect is optimal. For the sample infiltration parameter f0, the BP artificial neural network model has the lowest RSS value (0.0005), P-R maximum (0.99922) and R2 maximum (0.99845), and the fitting effect is optimal.

(2) Result Error Analysis: In order to facilitate the analysis of the relative error of the prediction results, the infiltration parameters are arranged in order from small to large. The relative error between the predicted and measured values of each infiltration parameter is shown in Figure 3. The relative error maximum, minimum and average values are shown in Table 7.

Table 7. Maximum value and the average value of the relative error between the measured value and the predicted value of the infiltration parameter of the sample

Parameters	Multiple linear model			Nonlinear model			BP neural network model		
	max	*min*	*mean*	*max*	*min*	*mean*	*max*	*min*	*mean*
k	0.392	0.001	0.152	0.301	0	0.071	0.243	0	0.036
α	0.394	0.013	0.175	0.372	0	0.096	0.197	0	0.056
f_0	0.203	0.00029	0.155	0.248	0	0.076	0.176	0	0.013

When the infiltration parameter k is predicted by the multivariate linear model, $0.001 \leq REk \leq 0.392$ and REkmean = 0.152. It can be seen from Figure 3 that as k value increases ($0 < k < 3.5$ cm/min), the error between the measured value and the predicted value increases. According to statistics, when k>2.3 cm/min, the relative error is greater than 20%, accounting for 75.23%. When using the nonlinear model to predict the infiltration parameter k, $0 \leq REk \leq 0.301$, REkmean=0.071, the

error between the measured value and the predicted value increases with the increase of the k value, which is consistent with the linear model prediction result. When using the BP artificial neural network model to predict the infiltration parameter k, 0 ≤ REk≤ 0.392 and REkmean = 0.036.

When the infiltration parameter α is predicted by the multivariate linear model, 0.013≤ Reα ≤0.394 and Reαmean = 0.175. When the infiltration parameter α is predicted by a multivariate nonlinear model, 0≤ Reα ≤0.372 and REαmean=0.096. When BP inductive neural network model was used to predict the infiltration parameter α, 0≤ Reα ≤0.197 and Reαmean = 0.056.

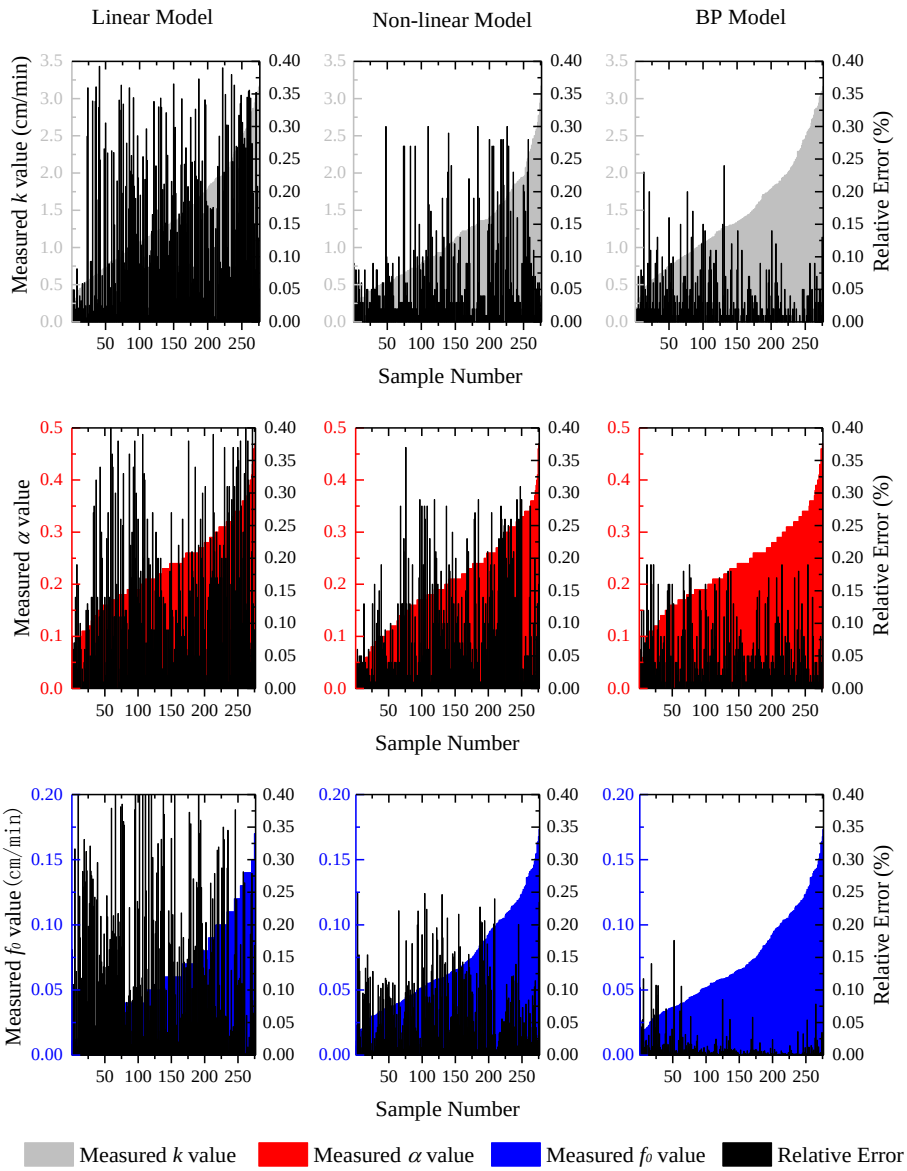

Figure 3. The relative error of prediction results of infiltration parameters of samples

When the infiltration parameter f0 is predicted by the multivariate linear model, 0.00029≤RE f0≤0.203 and RE f0mean = 0.155. When the infiltration parameter f0 is predicted by a multivariate nonlinear model, 0≤ RE f0 ≤0.248 and RE f0mean = 0.076. When the BP artificial neural network model is used to predict the infiltration parameter f0, 0≤ RE f0 ≤0.176 and RE f0mean=0.013.

For the three methods, the multivariate linear model is a simple superposition of the influencing factors, but cannot accurately reflect the influence of each factor on the whole. The forecast accuracy is lower than the nonlinear model and the BP neural network model, but the physical meaning Clear and easy to use. Compared with the multivariate linear model, the nonlinear model can reflect the

nonlinear relationship between the independent variable and the infiltration parameter to a certain extent. The physical meaning is clear, and the prediction accuracy is greatly improved compared with the multivariate linear model. Compared with the former two models, the BP neural network model has higher prediction accuracy and can accurately reflect the nonlinear relationship of various factors.

However, the model is complex in form and has high requirements on the user computer level. Therefore, the BP artificial neural network model has poor generalization.

(3) Comprehensive Error Analysis: The obtained k, α, and f0 values are substituted into the Kostiakov-Lewis model, and the fitted value of I90 (cumulative infiltration amount in 90 min) is obtained. The relative error of the I90 is obtained by comparing the predicted value with the measured value (Table 8).

Table 8. Analysis of the predict results of I90 of the sample

Samples	Measured	Multiple linear model		Nonlinear model		BP neural network model	
	I_{90}	Predicted I_{90}	*RE*	Predicted I_{90}	*RE*	Predicted I_{90}	*RE*
1	15.1070	13.3092	0.1190	14.8537		14.9128	0.01285
2	17.3600	17.9958	0.03662	16.9921		17.2641	0.005524
…	…	…	…	…	…	…	…
343	16.7500	16.3607	0.02324	16.9745		15.9062	0.05037
344	10.7120	11.1008	0.03629	10.4931		11.4339	0.06795
max	—	—	0.1549	—	0.1271	—	0.09842
min	—	—	0.00825	—	0.00001	—	0
mean	—	—	0.1105	—	0.09217	—	0.08005

It can be seen from Table 8 that the relative error of the multivariate linear model for predicting I90 is 0.00825≤ REI90 ≤0.1549 and RE I90mean = 0.1105. The relative error of I90 is predicted by the multivariate nonlinear model 0.00001≤ REI90 ≤0.1271 and RE I90mean = 0.09217. The relative error of I90 predicted by BP neural network model is 0≤ REI90 ≤0.09824 and RE I90mean = 0.08005. The prediction accuracy of the three models is within the acceptable range, indicating that all three models can achieve accurate prediction of I90.

4. Conclusions

(1) Soil infiltration parameters had great correlation of soil physical-chemical properties. The bulk density of 0-10cm and sand content of 0-20cm had negative effect in parameter k. The water content of 0-10cm and the organic matter of 0-20cm had positive effect in parameter k. The water content of 0-40cm, silt content and clay content of 0-20cm had negative effect in parameter α. The bulk density of 10-20cm and sand content of 0-40cm had positive effect in parameter α. The bulk density of 10-20cm , water content of 0-40cm and silt content of 0-40cm had negative effect in parameter f0. The bulk density of 20-40cm, sand content of 0-40cm and organic matter of 0-20cm had positive effect in parameter f0. The organic matter content had great influence in soil infiltration properties.

(2) The multivariate nonlinear model has the advantages of simple form, clear physical meaning and easy to use. Although the forecasting accuracy is lower than that of the BP artificial neural network model, it has perfected the basic data for scientific researchers and laid a solid foundation for the fragile ecological environment in the Loess Plateau.

Acknowledgments: This research was supported by the National Natural Science Foundation of China (40671081), Experimental Research Project of Irrigation Water Utilization Rate in Shanxi Provincial Water Resources Department.

References

1.GREEN, H., Studies on Soil Physics: Part II — The Permeability of an Ideal Soil to Air and Water. *J. Agri. Sci.*, **5**(1), 1912, 1-26.
2.KOSTIAKOV, A. N., On the dynamics of the coefficient of water percolation in soils and the

necessity of studying it from the dynamic point of view for the purposes of amelioration. *Trans. Sixth. Comm. Int. Soc. Soil Sci.,* **1**, 1932, 7-21.
3.PHILIP, J. R., The Theory of Infiltration: 4. Sorptivity and Algebraic Infiltration Equations. *Soil. Sci.,* **84**(3), 1957, 257-264.
4.HORTON, R. E., An approach toward a physical interpretation of infiltration-capacity 1. *Soil. Sci. soc. Am. J.*, ***5***(C), 1941, 399-417.
5.ELLIOTT, R., WALKER, W., Field evaluation of furrow infiltration and advance functions. *Trans. ASAE.*, **25**(2), 1982, 396-0400.
6.SHEPARD, J., WALLENDER, W., HOPMANS, J., One-point method for estimating furrow infiltration. *Trans. ASAE.,* **36**(2), 1993, 395-404.
7.MAHESHWARI, B. L., TURNER, A. K., MCMAHON, T. A., CAMPBELL, B. J., An optimization technique for estimating infiltration characteristics in border irrigation. *Agri. Water. manag.,* **13**(1), 1988, 13-24.
8.JIAO, X., WANG, W., LEI, Z., ZHANG, J., Improved Maheshiwari method for estimating infiltration parameters of soil. *J. Hydraul. Eng.,* **32**(1), 2001, 0062-0068.
9.ZHANG, X. M., WANG, G. X., XIANG-QUAN, H. U., WANG, Y. B., Nonlinear regression method for estimating infiltration parameters according to border irrigation data. *J. Hydraul. Eng.*, **36**(1), 2005, 28-34.
10.BOUMA, J., Using Soil Survey Data for Quantitative Land Evaluation. *Springer. N. Y.,* **9**, 1989, 177-213.
11.GHORBANI, M. A., SHAMSHIRBAND, S., HAGHI, D. Z., AZANI, A., BONAKDARI, H., EBTEHAJ, I., Application of firefly algorithm-based support vector machines for prediction of field capacity and permanent wilting point. *Soil. Till. Res.,* **172**, 2017, 32-38.
12.VEREECKEN, H., WEYNANTS, M., JAVAUX, M., PACHEPSKY, Y., SCHAAP, M. G., VAN-GENUCHTEN, M. T., Using Pedotransfer Functions to Estimate the van Genuchten-Mualem Soil Hydraulic Properties: A Review. *Vadose. Zone. J.,* **9**(4), 2010, 795-820.
13.BAGARELLO, V., PRIMA, S. D., IOVINO, M., Estimating saturated soil hydraulic conductivity by the near steady-state phase of a Beerkan infiltration test. *Geoderma.*, **303**, 2017, 70-77.
14.KARANDISH, F., ŠIMŮNEK, J., A comparison of numerical and machine-learning modeling of soil water content with limited input data. *J. Hydro.*, **543**, 2016, 892-909.
15.ZHAO, C., SHAO, M. A., JIA, X., NASIR, M., ZHANG, C., Using pedotransfer functions to estimate soil hydraulic conductivity in the Loess Plateau of China. *Catena.,* **143**(143), 2016, 1-6.
16.DE VOS, B., VAN MEIRVENNE, M., QUATAERT, P., DECKERS, J., MUYS, B., Predictive Quality of Pedotransfer Functions for Estimating Bulk Density of Forest Soils. *Soil. Sci. Soc. Am. J.,* **69**(2), 2005, 500-510.
17.XIANGSHENG, Y. I., GUOSHENG, L. I., YIN, Y. Y., Pedotransfer functions for estimating soil bulk density: A case study in the Three-River Headwater region of Qinghai Province, China. *Pedosphere.,* **26**(3), 2016, 362-373.
18.FERNÁNDEZ-UGALDE, O., TÓTH, G., Pedotransfer functions for predicting organic carbon in subsurface horizons of E uropean soils. *Eur. J. Soil Sci.,* **68**(5), 2017, 716-725.
19.FRANZLUEBBERS, A. J., Achieving soil organic carbon sequestration with conservation agricultural systems in the southeastern United States. *Soil. Sci. Soc. Am. J.,* **74**(2), 2010, 347-357.
20.WIESMEIER, M., SPÖRLEIN, P., GEUß, U., HANGEN, E., HAUG, S., REISCHL, A., SCHILLING, B., VON-LUTZOW, M., KÖGEL-KNABNER, I., Soil organic carbon stocks in southeast Germany (Bavaria) as affected by land use, soil type and sampling depth. *Glob. Change. Biol.*, **18**(7), 2012, 2233-2245.
21.GHORBANI-DASHTAKI, S., HOMAEE, M., LOISKANDL, W., Towards using pedotransfer functions for estimating infiltration parameters. *Hydrolog. Sci. J.,* **61**(8), 2016, 1477-1488.
22.OMUTO, T. C., MINASNY, B., MCBRATNEY, A. B., BIAMAH, E. K., Nonlinear mixed effect modelling for improved estimation of water retention and infiltration parameters. *J. Hydro.,* **330**(3),

2006, 748-758.
23.PARCHAMI-ARAGHI, F., MIRLATIFI, S. M., DASHTAKI, S. G., MAHDIAN, M. H., Point estimation of soil water infiltration process using Artificial Neural Networks for some calcareous soils. *J. Hydro.*, **481**(5), 2013, 35-47.
24.ZENG, L., CHEN, G., CHEN, H., Comparative Study on Flow-Accelerated Corrosion and Erosion–Corrosion at a 90° Carbon Steel Bend. *Materials*, **13**(7), 2020, 1780-1796.
25.CHEN, H., FAN, D., HUANG, J., HUANG, W., ZHANG, G., HUANG, L., Finite Element Analysis Model on Ultrasonic Phased Array Technique for Material Defect Time of Flight Diffraction Detection. *Sci. Adv. Mater.*, **12**(5), 2020, 665-675.
26.CHENG, Y., SONG, Z., JIN, J., WANG, J., WANG, T., Experimental study on stress wave attenuation and energy dissipation of sandstone under full deformation condition. *Arab. J. Geosci.*, **12**(23), 2019, 736-749.
27.WANG, H., WANG, J., LU, H., BO, G., ZHANG, X., CAO, Y., LIU, L., ZHANG, J., ZHANG, W., Analysis of coating electrode characteristics in the process of removing pollutants from wastewater. *Fresenius. Environ. Bull.,* **29**(2), 2020, 715-721.
28.HAIBIN, L., ZHENLING, L., Recycling utilization patterns of coal mining waste in China. *Resour. Conserv. Recycl.*, **54**(12), 2010, 1331-1340.
29.GU, F., GUO, J., ZHANG, W., SUMMERS, P. A., HALL, P., From waste plastics to industrial raw materials: A life cycle assessment of mechanical plastic recycling practice based on a real-world case study. *Sci. Total. Environ.*, **601**, 2017, 1192-1207.
30.LIU, Z., FENG, J., WANG, J., Resource-Constrained Innovation Method for Sustainability: Application of Morphological Analysis and TRIZ Inventive Principles. *Sustainability*, **12**(3), 2020, 917-939.
31.WANG, M., ZHANG, D., CHENG, Y., TAN, S. K., Assessing performance of porous pavements and bioretention cells for stormwater management in response to probable climatic changes. *J. Environ. Manage.*, **243**, 2019, 157-167.
32.WANG, H., AN, X., ZHANG, Z., Effect of advanced treatment on ammonia nitrogen contained in secondary effluent from wastewater treatment plant. *Fresenius. Environ. Bull.*, **27**(4), 2018, 2043-2050.
33.WANG, H., ZHONG, H., BO, G., Existing forms and changes of nitrogen inside of horizontal subsurface constructed wetlands. *Environ. Sci. Poll. Res.*, **25**(1), 2018, 771-781.
34.QUAN, Q., HAO, Z., XIFENG, H., JINGCHUN, L., Research on water temperature prediction based on improved support vector regression. *Neur. Comp. App.*, 2020, 1-10.
25.LIU, Y. X., YANG, C. N., SUN, Q. D., WU, S. Y., LIN, S. S., CHOU, Y. S., Enhanced embedding capacity for the SMSD-based data-hiding method. *Signal Processing: Image. Commun.*, **78**, 2019, 216-222.
36.CAO, Y., WANG, Q., FAN, Q., NOJAVAN, S., JERMSITTIPARSERT, K., Risk-constrained stochastic power procurement of storage-based large electricity consumer. *J. Energy. Stor.*, **28**, 2020, 101183-101192.
37.CAO, Y., LI, Y., ZHANG, G., JERMSITTIPARSERT, K., NASSERI, M., An efficient terminal voltage control for PEMFC based on an improved version of whale optimization algorithm. *Energy Reports*, **6**, 2020, 530-542.
38.GU, F., GUO, J., YAO, X., SUMMERS, P. A., WIDIJATMOKO, S. D., HALL, P., An investigation of the current status of recycling spent lithium-ion batteries from consumer electronics in China. *J. Clean. Prod.*, **161**, 2017, 765-780.
39.RAHMATI, M., Reliable and accurate point-based prediction of cumulative infiltration using soil readily available characteristics: a comparison between GMDH, ANN, and MLR. *J. Hydro.*, **551**, 2017, 81-91.

Manuscript received: 17.03.2020